

## Erosion as a Factor of Transformation of Soil Radioactive Contamination in the Basin of the Shchekino Reservoir (Tula Region)

V. N. Golosov<sup>a, b, c</sup>, M. M. Ivanov<sup>a, b</sup>, A. S. Tsyplenkov<sup>a</sup>, M. A. Ivanov<sup>c</sup>, Y. Wakiyama<sup>d</sup>,  
A. V. Konoplev<sup>d</sup>, E. A. Konstantinov<sup>b</sup>, and N. N. Ivanova<sup>a, \*</sup>

<sup>a</sup>Lomonosov Moscow State University, Moscow, 119991 Russia

<sup>b</sup>Institute of Geography, Russian Academy of Sciences, Moscow, 119017 Russia

<sup>c</sup>Kazan Federal University, Kazan, 420008 Russia

<sup>d</sup>Institute of Environment Radioactivity, Fukushima University, Kanayagawa, Fukushima, 1960–1296 Japan

\*e-mail: nadine\_iv@mail.ru

Received April 30, 2020; revised June 16, 2020; accepted July 13, 2020

**Abstract**—Redistribution of sediments and Chernobyl-derived <sup>137</sup>Cs transported with them were estimated using a set of field methods and erosion model calculations for the Shchekino reservoir (Tula region) catchment, and changes in the contents of <sup>137</sup>Cs in soils of various types that occurred over 1986–2018 were determined. The rate of snowmelt soil erosion on arable land during this period has decreased by about a half in comparison with that in 1960–1985 due to a reduction in soil freezing depth in winter. The rainfall erosion rate increased by about a third between 1986–2003 due to an increase in the rainfall erosivity index; after that, it tended to decrease synchronously with a decrease in the rainfall erosivity. The total average annual soil loss related to water erosion varies in the range of 1.3–1.6 t ha<sup>-1</sup> depending on the soil type. The erosional loss of <sup>137</sup>Cs from arable land averaged 1.5–2% of its total inventory, which decreased by more than a half in comparison with the initial inventory in May 1986 due to natural decay. On 0.4% of the arable land with maximum rates of erosion, the decrease in the <sup>137</sup>Cs inventory reached 12–40% from the initial inventory. More than 90% of <sup>137</sup>Cs washed away with sediments from arable lands were redeposited along the transportation pathway from arable fields to permanent streams. The total soil <sup>137</sup>Cs inventory exceeded its initial inventory at the time of fallout from the atmosphere in May 1986 in the bottoms of hollows in areas from the lower edge of the arable land to the upper reaches of dry first-order valleys due to high sedimentation rates. The <sup>137</sup>Cs inventory exceeded the lower threshold of permissible radioactive contamination of soils (37 kBq m<sup>-2</sup>) also in some other sediment sinks (bottoms of dry valleys, foot of plowed slopes, and a low floodplain of rivers) due to the accumulation of contaminated sediments.

**Keywords:** radioactive contamination, snowmelt erosion, rainfall erosion, <sup>137</sup>Cs inventory, sediment redistribution, Luvic Chernic Phaeozems, Luvic Greyzemic Chernic Phaeozems, Luvic Retic Greyzem Phaeozems, Stagnic Phaeozems (Colluvic, Pachic)

**DOI:** 10.1134/S106422932102006X

### INTRODUCTION

Soils of a part of Europe were radioactively contaminated (mainly, with <sup>137</sup>Cs) after the Chernobyl disaster at the end of April 1986 [28]. On a larger part of polluted territory, the levels of radioactive contamination of soils did not exceed the permissible values and were comparable in magnitude with the pollution from <sup>137</sup>Cs global fallout as a result of nuclear explosions in the atmosphere since the beginning of the 1950s and until 1963. However, locally, areas with contamination levels exceeding the maximum permissible level were formed, including those in the European part of Russia. For example, in the southern half of Tula region, the maximum fallout of <sup>137</sup>Cs and other radionuclides was observed in the area extending from Chernskii to Bogoroditskii districts; this area is known

as the Plavsk cesium spot (Fig. 1). It is found in the agricultural region with a high proportion of arable lands. The content of <sup>137</sup>Cs, which is quickly and firmly fixed on soil particles, determines the level of radioactive contamination of soils [3, 32]. In regions with a high proportion of arable lands, erosion-accumulative processes are the main mechanism for the subsequent redistribution of radionuclides within river basins [31]. In the north of the forest-steppe zone of the European part of Russia, wind erosion is not developed [12]. Snowmelt erosion in spring and rainfall erosion in summer and fall play the major role in the lateral migration of <sup>137</sup>Cs. Over more than 30 years that have passed since the Chernobyl disaster, the content of <sup>137</sup>Cs in soils has already been halved due to natural decay (the half-life period of <sup>137</sup>Cs is 30.2 years).

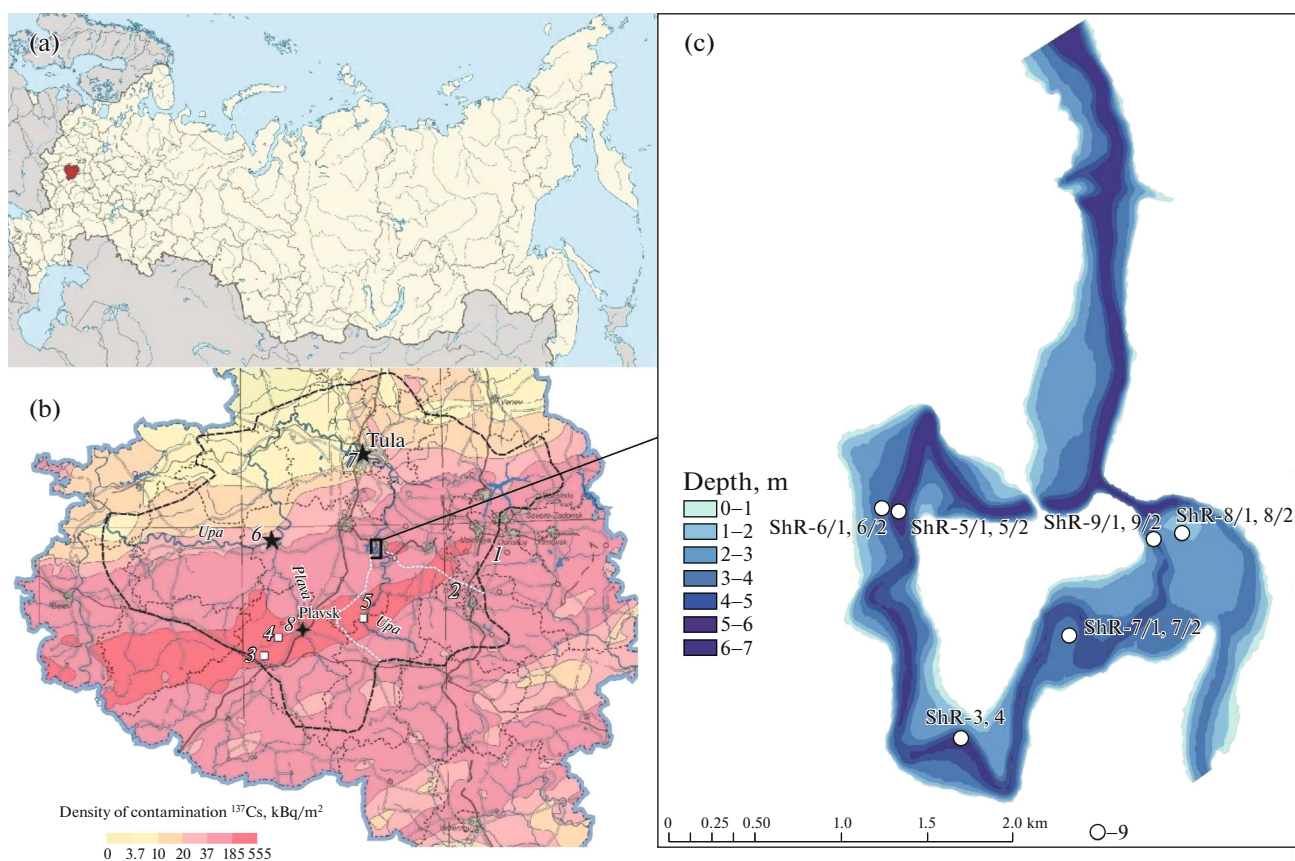


**Fig. 1.** Research area, location of gauging stations, weather stations, and sampling points for soil and bottom sediments: (a) location of Tula region; (b) map of radioactive contamination of Tula oblast in 1986 [4] ((1) boundary of the Upa River basin, (2) catchment of the Shchekino reservoir; soil sampling sites: (3) grassed bottom of the hollow and plowed slope, (4 and 5) floodplains of the Lokna and  $\text{Plavsk}$  rivers, respectively; gauging stations on the Upa River: (6) Orlovo, (7) Tula; (8) weather station in  $\text{Plavsk}$ ); and (c) bathymetric map of the Shchekino reservoir ((9) sampling points of bottom sediment cores).

The water erosion contributes to the redistribution of washed off soil particles with  $^{137}\text{Cs}$  fixed on them within river catchments. As a result, secondary pollution areas are formed, where the total  $^{137}\text{Cs}$  inventory exceeds the levels of its initial deposition [22, 45]. These areas include unplowed lower parts of slopes, bottoms of dry valleys, floodplains, and water bodies, in which the accumulation of  $^{137}\text{Cs}$  transported with soil particles takes place [36, 37, 39, 41, 47].

Available estimates of  $^{137}\text{Cs}$  redistribution are mainly based on the use of erosion models, or their combined use with actual measurements of the total  $^{137}\text{Cs}$  inventory in the areas of erosion and accumulation [31]. In some cases, for the catchments of small ponds, the  $^{137}\text{Cs}$  budget was assessed taking into account its accumulation in bottom sediments [35]. At the same time, no quantitative assessments of  $^{137}\text{Cs}$  redistribution for catchments of large reservoirs have been carried out so far.

This study aims at a quantitative assessment of the transformation of the field of radioactive soil contamination in 32 years after the Chernobyl disaster for the

catchment of the Shchekino reservoir under the impact of erosion-accumulative processes.

## OBJECTS AND METHODS

**Study area.** The Shchekino water reservoir was created in 1950 in the upper reaches of the Upa River as a cooling pond of the Shchekinskaya electric power station. Its catchment (1350 km<sup>2</sup>) is found southeast of the center of Tula oblast (Fig. 1), in the agricultural region with a predominance of arable land and the absence of large settlements.

According to the Köppen–Geiger climate classification, the investigated part of the Upa River basin is located in the humid continental (Dfb) climate zone without dry season and with hot summer. The mean annual precipitation slightly decreases from the northwest to the southeast from 630 to 592 mm with about 460 mm in the warm season. The upper reaches of the Upa River lie near the main divide between the Volga and Don River basins. The studied territory is a part of the eastern slope of the Central Russian Upland and it

is characterized by a relatively slightly dissected topography with extensive nearly level watersheds. The maximum relative elevation of the relief is observed in the western part of the Upa River basin, where the river sharply turns to the northeast towards the Shchekino reservoir. This part of the basin was most heavily contaminated after the Chernobyl disaster (Fig. 1b). The network of permanent streams includes the Upa River, its large right-bank tributary—the Uperta River—and their confluents. The soil cover of the basin consists of leached chernozems (Luvic Chernic Phaeozems), podzolized chernozems (Luvic Greyzemic Chernic Phaeozems), and dark gray forest soils (Luvic Retic Greyzemic Phaeozems) on the interfluvies covered with loesslike calcareous loam as the parent material is [16]. Leached meadow chernozemic soils (Stagnic Phaeozems (Colluvic, Pachic)) developed from colluvial and alluvial sediments predominate in the bottoms of the valleys of the fluvial network. Soddy alluvial soils (Umbric Fluvisols) of floodplains extend along river channels as narrow intermittent strips.

Earlier large-scale studies of the transformation of the initial radioactive contamination field within the Plavsk cesium spot showed its high spatial variability [19], which becomes hidden on the map of radioactive contamination of Tula oblast because of cartographic generalization. In this work, we do not take into account spatial differences in the initial soil contamination over the studied catchment, because the entire catchment was characterized by the high initial contamination level exceeding maximum permissible values and being higher than 37 kBq/m<sup>2</sup> [2].

**Methods.** To assess changes in the degree of soil contamination within the Shchekino reservoir catchment for the period from 1986 to 2018, we used the approach based on the calculation of the <sup>137</sup>Cs inventory for the main types of soils and for different elements of the fluvial relief. The reliability of the obtained estimates is provided by the possibility of checking the calculated changes of the total <sup>137</sup>Cs inventory in soils of various types on the basis of their comparison with data on the <sup>137</sup>Cs inventory in bottom sediments of the Shchekino reservoir.

At the initial stage of the research, the dynamics of changes in the arable land area were assessed. For this purpose, high-resolution satellite images obtained in 1985, 2003, and 2018 were interpreted. Level-2 Data Products—Surface Reflectance Landsat 5 (Thematic Mapper, TM), Landsat 7 (Enhanced Thematic Mapper Plus (ETM+)), and Landsat 8 (Operational Land Imager, OLI) images—were used as the initial data. The images of different seasons in snowless time were chosen for the entire catchment. Their interpretation was based on the methodology applied in the CORINE Land Cover 2000 (CLC2000) project [25, 26] adjusted for the regional specificity and goals of our study. For mapping arable fields, we used the method of visual

interpretation and subsequent manual digitization. For other land uses, we used the automatic classification by the Random Forest method with the number of trees equal to 100. Thus, three vector layers of land use maps for different years were obtained. Their overlay showed the areas of reduction and increase of arable land and other land categories for the estimated time intervals. The calculation of the areas of used and abandoned arable land was carried out in the MapInfo program. A more detailed description of the methods of image interpretation is given in [10].

To calculate rainfall erosion, the revised universal soil loss equation (RUSLE) was used [45]:

$$Y = R K L S C P, \quad (1)$$

where  $Y$  is the annual soil loss from unit area, t/ha yr;  $R$  is the rainfall erosivity factor, MJ mm/(h ha yr);  $K$  is the soil erodibility factor, t h/(MJ mm);  $LS$  is the topographic factor (slope length and slope gradient), dimensionless;  $C$  is the cover and management factor, dimensionless; and  $P$  is the erosion control efficiency factor, dimensionless.

As erosion control measures have not been performed on arable slopes of the Shchekino reservoir catchment, the  $P$  factor was taken equal to 1 in the calculations. For all the computational models, the ALOS World 3D (AW3D30) Version 2.2 global digital elevation model (GDEM) [54] with a spatial resolution of  $1 \times 1$  s, which is equivalent to  $30 \times 30$  m, was applied after the hydrological correction with the Fill Sinks algorithm [49] implemented in QGIS 3.6.2. The minimum slope, at which runoff is possible, was left at the default of  $0.01^\circ$ . The DEM of this resolution is considered sufficient for modeling soil erosion [38, 52].

The calculation of the topographic  $LS$  factor was performed in QGIS 3.6.2 using the  $LS$  field-based modulus from SAGA GIS [27] according to the recommendations [43]. This algorithm is based on the equation proposed in [30]:

$$LS = (m + 1) \left( \frac{U}{L_0} \right)^m \left( \frac{\sin \beta}{S_0} \right)^n, \quad (2)$$

where  $LS$  is the topographic factor, dimensionless;  $U$  is the upper lying catchment area referred to the flow width, m<sup>2</sup>/m;  $L_0$  and  $S_0$  are the length and steepness of the standard Wischmeier—Smith drainage area [51];  $\beta$  is slope steepness, degrees;  $m$  (0.4–0.6) and  $n$  (1.0–1.3) are empirical parameters depending on the prevailing type of erosion (sheet or rill erosion). Slopes  $>26.6^\circ$  were excluded from the calculations, because they are associated with artifacts of the GDEM.

Factor  $C$  values vary over time depending on the set of crops sown on arable land in particular time. It was impossible to reconstruct actual crop rotations for the Shchekino catchment for the entire period since 1986. Reliable data on the ratio of cultivated areas under different crops were available only for the Tula region as a whole. In the long-term perspective, average calcu-

lated values of the  $C$  factor for arable lands vary very slightly in the range of 0.32–0.33. For other land use types,  $C$  values were taken from the generalized data [23, 43] (Table S1).

To calculate the soil erodibility factor and its distribution within the studied catchment, the soil map on a scale of 1 : 2.5 M and tabulated data from [9] were used. The calculation of the soil erodibility factor coefficient was carried out using the Williams equations [50] (see Supplementary material).

The global rainfall erosivity database created for Russia and based on 30-min precipitation data from 1961 to 1983 was used to assess the distribution of the rainfall erosivity ( $R$ ) factor for the Shchekino catchment [42]. The weighted average  $R$  value for the catchment is 306 MJ mm/(h ha year) (SD = 4.02); minimum values ( $R = 294$  MJ mm/(h ha year)) are observed in the southeastern part, and maximum values ( $R_{\max} = 319$  MJ mm/(h ha year)) are in the western part of the catchment. Taking into account the fact that the spatial variability of this parameter is low and, in general, lies within the error of measurements, this value was taken as a constant in space, but its changes over time were taken into account.

There are no weather stations in the catchment; the nearest station is located in the Plavsk to the west of the Shchekino reservoir. Daily information on precipitation and air temperature was collected for the period 1986–2018 in the AISORI database [1]. Empirical formulas [40] derived for each type of Köppen–Geiger climate were used to calculate  $R$  for the period after 1986 [45]:

$$\log R = -0.5 + 0.266 \log P + 3.11 \lg SDII - 0.131 \lg Z, \quad (3)$$

where  $R$  is the rainfall erosivity, MJ mm/(h ha year);  $P$  is the annual precipitation, mm;  $SDII$  is an elementary index of precipitation intensity equal to the ratio of annual precipitation  $P$  to the number of days with liquid precipitation  $> 1$  mm, mm/day;  $Z$  is the absolute elevation of the weather station, m. Air temperature of  $+2^\circ\text{C}$  was used to separate precipitation into liquid and solid forms according to the recommendations [18].

The sediment delivery ratio proposed in [24] was calculated using the DEM data for each  $i$  cell to assess the redistribution of sediments washed away from arable fields and transported together with  $^{137}\text{Cs}$  to the upper parts of the fluvial network up to the channels of permanent streams:

$$SDR_i = \frac{SDR_{\max}}{1 + \exp\left(\frac{IC_0 - IC_i}{k}\right)}, \quad (4)$$

where  $SDR_{\max}$  is the theoretical maximum of sediment delivery ratio;  $IC_0$  and  $k$  are calibration coefficients that determine the shape of the function  $SDR = f(IC)$ ; and  $IC_i$  is the index of connectivity of the upper and

lower reaches of the slope calculated for each element of the hydrographic network by the formula:

$$IC = \log_{10} \left( \frac{D_{up}}{D_{dn}} \right), \quad (5)$$

where  $D_{up}$  is a parameter characterizing the potentially possible amount of sediment that can be transported from the erosion zone to the transport zone on the slope,  $D_{dn}$  is the weighted length of the transport zone on the slope, which includes all the factors that can affect the retention of an elementary particle [48]. These components of the equation depend on the mean slope, the area of the upper lying catchment, and the  $C$  factor (from the RUSLE equation).

$$D_{up} = \bar{C} \bar{S} \sqrt{A}, \quad (6)$$

where  $C$  is the average value of the cover and management factor from the RUSLE equation for the upper part of the catchment;  $S$  is average slope of the upper part of the slope, m/m; and  $A$  is the area of the erosion zone on the slope,  $\text{m}^2$ .

$$D_{dn} = \sum_i \frac{d_i}{C_i S_i}, \quad (7)$$

where  $d_i$  is the thalweg length of the flow inside each  $i$  cell of the raster, m; and  $C_i$  and  $S_i$  are the values of the cover and management factor and slope steepness for each  $i$  cell, respectively.

Monitoring data on the rainfall erosion are absent for the center of the European part of Russia. As for snowmelt erosion, the results of stationary observations on plowed slopes in the center of the Russian Plain lasting for 9–12 years are available [5, 8, 14]. They were used to estimate average rates of snowmelt erosion. According to the data obtained at the Kursk Biosphere Station in center of the Central Russian Upland with leached and typical chernozems, the average long-term snowmelt erosion reaches 0.5 t/(ha yr) [8]. Studies of the snowmelt runoff on plowed catchments of the experimental site of the Dokuchaev Soil Science Institute (in the north of the Central Russian Upland with gray forest soils) make it possible to estimate soil losses on predominantly convex southern slopes of  $1^\circ$ – $5^\circ$  at 5.4 t/(ha yr) [5]. It should be noted that the results of observations of snowmelt erosion in the north of the Central Russian Upland [5] reflect the values of soil loss from the slopes of “warm” exposures, which are twice as high as the rate of snowmelt erosion on the slopes of “cold” exposures [6, 13]. Also, a decrease in the surface runoff coefficient since the 1990s because of the increasing air temperatures in winter and decreasing depth of soil freezing should be taken into account. Since the beginning of the 2000s, years with the absence of surface snowmelt runoff have been predominant in this area [15, 20]. This is confirmed by data on the dynamics of the depth of soil freezing and maximum flood levels in the Upa River basin (Fig. S3). Finally, an analysis of observation data of the mid-

1980s, including observations of rainfall and snowmelt runoff and soil erosion on runoff plots in the center of the East European Plain allows us to estimate the average annual intensity of soil loss at 1–1.5 t/(ha yr) [6]. As a result, taking into account the actual climate changes since 1990, which reduced the frequency of formation of snowmelt runoff flows on arable land; two options were used in calculating the total soil losses during the snowmelt period. The first one assumed the loss of 1 t/(ha yr) in years with the formation of snowmelt runoff on the slopes, the number of which according to hydrometeorological data was 11 years in 1987–2003 and 6 years in 2004–2018. In the second option, the average annual soil loss of 0.5 t/(ha yr) was used for the entire period from 1987.

Layer-by-layer sampling was carried out from test areas of 15 × 15 cm with a step of 3 cm to a depth of 60–80 cm to determine the rate of sediment accumulation and changes in the <sup>137</sup>Cs inventory in the redeposition zones (bottoms of hollows and dry valleys, river floodplains). After the spring flood, freshly deposited alluvial sediments were sampled to determine the <sup>137</sup>Cs content in them. Soil samples were dried at 105°C, comminuted, and sieved through a 1-mm mesh in the laboratory.

Bottom sediments were sampled with a piston sampler to determine the total volumes of sediment and <sup>137</sup>Cs accumulation in the Shchekino reservoir. Sampling points were chosen on the basis of the depth map [11]. In the upper part of the reservoir, 12 columns were taken from the ice. Sampling in the lower part of the reservoir located next to the power station was not carried out because of safety reasons due to the small thickness of the ice. The collected columns were packed in cellophane film, frozen, and delivered to the laboratory. In the laboratory, the sediment columns were divided into 2- and 5-cm-long samples for consolidated and for weakly consolidated sediments, respectively. Then, the samples were weighed, dried at 105°C for 8 h, and weighed again to determine the water content and calculate the density of the dry samples. After that, samples were ground and sieved through a 2-mm mesh.

Measurements of <sup>137</sup>Cs concentrations in prepared samples of soils, alluvial sediments on floodplains, and bottom sediments were carried out on a coaxial germanium gamma-spectrometer (Green Star Instruments (SKS-07 (09) P-G-R, Russia)) with a relative error of specific activity of 5–10%. Preparation (drying, homogenization) and gamma-spectrometric analysis of soil samples were performed in the Makka-veev Laboratory of Soil Erosion and Fluvial Processes of the Faculty of Geography of Lomonosov Moscow State University.

Additionally, particle size distribution of bottom sediments was determined by laser diffractometry on a Malvern Mastersizer 3000 particle size analyzer. The

particle size distribution was calculated by the Fraunhofer diffraction model.

Soil freezing depth data according to the Plavsk weather station and data on the maximum flood levels and water discharges, and sediment discharges in the Upa River according to data of the Tula and Orlovo hydrological stations for 1987–2018 were also collected.

## RESULTS

In general, within the Shchekino reservoir catchment, soils of the chernozemic type of soil formation occupy about 78% of the total catchment area. Dark gray forest soils locally occur mainly in the northwestern dissected part of the catchment. Leached meadow chernozemic soils occupy bottoms of river valleys and balkas and are also locally found on slopes of the interfluves. Their share is minimal compared to other soil types.

Since the 1990s, the plowed area in the Shchekino catchment have been gradually decreasing. From 1985 to 2018, it decreased from 71.3 to 61.2% of the total catchment area with a simultaneous increase in the percent of grassland (Table 2). Judging from the temporal changes in the topographic factor for different soil types, cropland abandoning was caused not by the exclusion of the steepest slopes from the arable land, but by other reasons (possibly, transport accessibility of the fields). Arable fields on podzolized Chernozems and meadow chernozemic soils were abandoned to a lesser extent. At the same time, the share of meadows increased by about 9% over the same period.

According to the erosion model, rainfall erosion on arable land increased from 0.65 t/(ha yr) in 1985 to 1.15 t/(ha yr) by the beginning of the 2000s due to an increase in the rainfall erosivity factor (*R*) by more than 1.5 times. However, by 2018, the rainfall erosion rate decreased to 0.95 t/(ha yr) because of a decrease in the rainfall erosivity factor (Table S4).

The increase in *R* was associated with an increase in the annual amount of liquid precipitation (Fig. S4). A similar trend was typical for the center of the Central Russian Upland [34]. At the same time, the changes in the rate of soil erosion rate for leached Chernozems in general (Table 3), for which the area of unmanaged fallow reached maximum in 2003, were also affected by the higher values of the topographic factor for the remaining arable land (Table 2).

In the assessment of the proportion of sediments of rainstorm erosion washed off from arable land and transported by temporary flows to permanent streams, it was taken into account that some part of the sediment is intercepted in the ponds created in the upper reaches of the fluvial network (Fig. 2). According to our estimates, only 3% of the sediments washed away from the arable land during the runoff-forming rainfalls entered permanent streams (Table 4). This corre-

**Table 1.** Percentage ratio of different soil types, mean ( $LS_{\text{mean}}$ ) and median ( $LS_{\text{med}}$ ) values of their topographic factor in the catchment of the Shchekino reservoir

Soil type	Area, km <sup>2</sup>	Share of the total catchment area, %	$LS_{\text{mean}}$	$LS_{\text{med}}$
Stagnic Phaeozems (Colluvic, Pachic)	48	3.6	1.82	0.68
Luvic Retic Greyzemic Phaeozems	242	18.4	3.29	1.33
Luvic Chernic Phaeozems	410	30	2.41	0.86
Luvic Greyzemic Chernic Phaeozems	650	48	3.05	1.07

**Table 2.** Arable land areas and the topographic factor for arable land sites with different soil types and their changes in time for the catchment of the Shchekino reservoir

Year	Soil type	$LS_{\text{mean}}$	$LS_{\text{med}}$	Arable land area, km <sup>2</sup>	Arable land, % of the total catchment area
1985	Stagnic Phaeozems (Colluvic, Pachic)	1.09	0.60	962	71.3
	Luvic Retic Greyzemic Phaeozems	2.00	1.16		
	Luvic Chernic Phaeozems	1.31	0.70		
	Luvic Greyzemic Chernic Phaeozems	1.70	0.89		
2003	Stagnic Phaeozems (Colluvic, Pachic)	1.13	0.60	920	65.4
	Luvic Retic Greyzemic Phaeozems	2.17	1.19		
	Luvic Chernic Phaeozems	1.53	0.76		
	Luvic Greyzemic Chernic Phaeozems	1.80	0.91		
2018	Stagnic Phaeozems (Colluvic, Pachic)	1.05	0.59	846	61.2
	Luvic Retic Greyzemic Phaeozems	1.98	1.18		
	Luvic Chernic Phaeozems	1.34	0.73		
	Luvic Greyzemic Chernic Phaeozems	1.67	0.90		

**Table 3.** Average annual rainstorm erosion rates in the catchment of the Shchekino reservoir for different soil types in 1985, 2003, and 2008 (average for all land use types)

Soil	Area, km <sup>2</sup> (%)	Weighted average calculated losses, t/(ha year)		
		1985	2003	2018
Luvic Greyzemic Chernic Phaeozems	410 (30)	0.57	0.93	0.8
Luvic Retic Greyzemic Phaeozems	242 (18.4)	0.62	0.97	0.81
Stagnic Phaeozems (Colluvic, Pachic)	48 (3.6)	0.78	1.12	1.18
Luvic Chernic Phaeozems	650 (48)	0.42	0.75	0.51

sponds to the sediment delivery ratio by rainstorm erosion for river basins of plain territories [29].

The total soil loss from the snowmelt erosion is more than two times lower than that from the rainfall erosion (Table 4). This is caused by a decrease in surface runoff from slopes during snow melting because of a decrease in the soil freezing depth and an increase in the number of winter thaws [15]. Empirical data obtained for the catchment of the Protva River (the Oka River basin) and based on a combination of direct observations of sediment washout during snow melting and analysis of the structure of the upper parts of the fluvial network were used to estimate the volume of sediment eroded

during the formation of snowmelt runoff on the cultivated lands and supplied to permanent streams [7]. According to these data, permanent streams receive 24% of the total volume of sediment washed away from the arable land during the snowmelt runoff.

According to the calculation based on the estimates of the actual volumes and density of bottom sediments, the sediment mass accumulated in the Shchekino reservoir over 1986–2018 was 410 000 tons. The calculations did not take into account the sediments deposited in the lower third of the reservoir downstream from the artificial canal (Fig. 1c), and a part of the suspended sediment carried beyond the reservoir

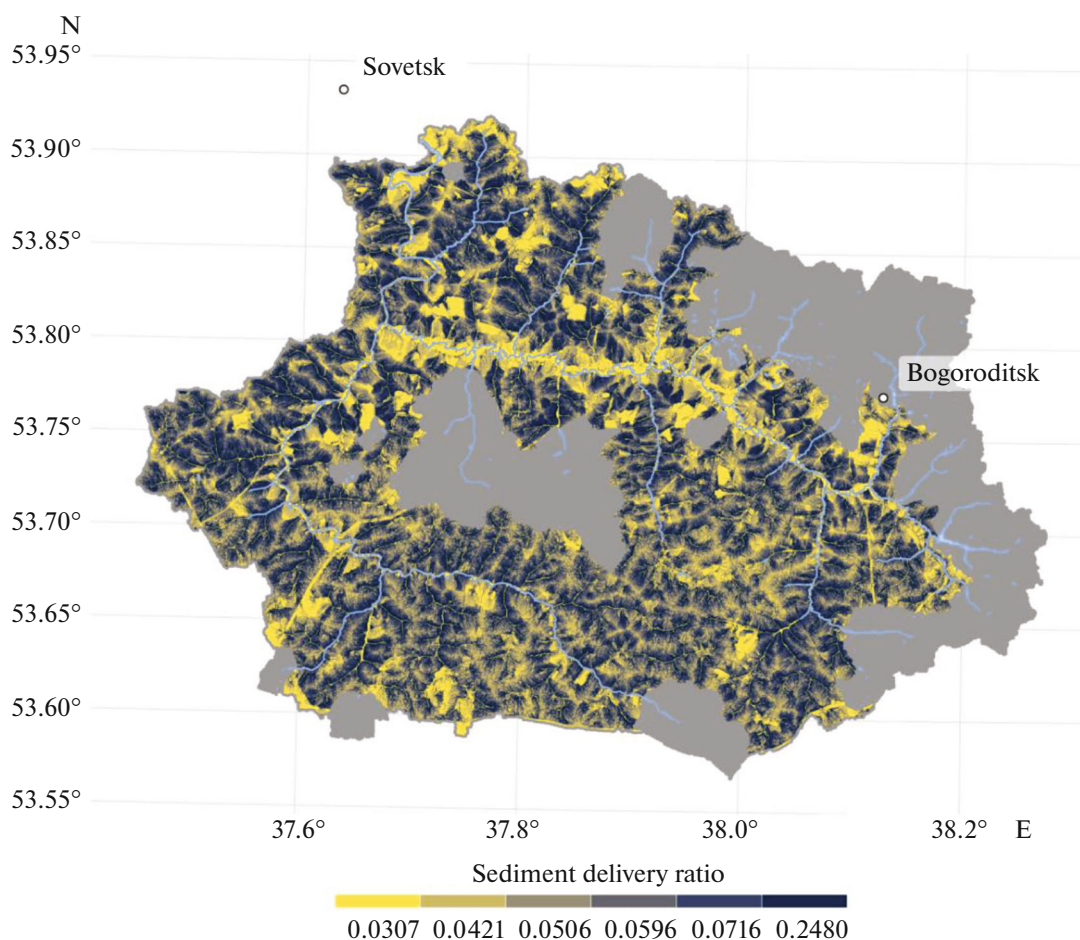


**Fig. 2.** Schematic map of the calculated sediment delivery ratio into permanent streams of the Shchekino reservoir basin formed during rainfall erosion. Catchments of ponds intercepting sediment runoff from the slopes are highlighted in gray.

**Table 4.** Quantitative estimates of the redistribution of sediments washed away from the slopes and redeposited along the transportation path to permanent streams in the Shchekino reservoir basin during the post-Chernobyl period

Period, years	Sediment mass, 10 <sup>3</sup> t		
	washed away from catchment	deposited along the transportation path from arable land to streams	delivered to permanent streams
Rainfall erosion			
1986–2003	1676.7	1626.4	50.3
2004–2018	1550	1509.5	46.5
Total 1986–2018	3226.7	3135.9	96.8
Snowmelt erosion			
1987–2003	1012/782*	769.1/594.3	242.9/187.7
2004–2018	552/634.5	419.5/482.2	132.5/152.3
Total 1986–2018	1564/1416.5	1188.8/1076.5	375.4/340
Total erosion (rainfall + snowmelt erosion)			
1987–2003	2686/2458.7	2595.5/2220.7	293.2/238
2004–2018	2102/2184.5	1929/1991.7	179/198.8
<b>Total</b>	<b>4780/4643.2</b>	<b>4525.5/4212.4</b>	<b>472.2/436.8</b>

\* Above the line, soil loss during snow melting calculated taking into account data on soil freezing and maximum flood levels; below the line, soil loss during snow melting calculated taking into account the average rate snowmelt erosion in 1987–2018 (0.5 t/(ha year)).

during regular water discharge, which is performed to maintain the water level at the water intake. The average  $^{137}\text{Cs}$  concentration in bottom sediments accumulated after 1986 was 463 Bq/kg.

## DISCUSSION

The obtained independent estimates of the mass of bottom sediments in the Shchekino reservoir (410 000 tons) and the mass of eroded sediments transported by temporary flows to the river network in 1986–2018 (454 000 tons) are comparable, which indicates a satisfactory accuracy of calculations of the sediment redistribution in the course of transportation from arable slopes to the bottoms of river valleys. Sediments washed off from the catchment are known to be the main source of alluvial sediments in river basins with a high proportion of arable land [17]. It should be noted that our estimates do not take into account channel erosion and sediment accumulation on the floodplain, which are also components of sediment budget of river catchments [7]. It is assumed that their contributions to the total sediment budget are close in magnitude, but, being different in sign, they are mutually compensated. The results of interpretation of satellite images and field surveys of rivers in the Shchekino reservoir catchment attest to a small number of areas of active erosion of river banks. The rate of sediment accumulation on the floodplain, according to the data for the low floodplain of the Upa River (Fig. 3e) are comparable to the rates of accumulation on the Lokna River (Fig. 3f) located within the Plavsk cesium spot [39] (Fig. 1b). The main part of sediments accumulates on the surface of narrow (2–5 m) fragments of a low floodplain, while the rates of material deposition and  $^{137}\text{Cs}$  accumulation on the medium-high and high floodplains of rivers in the Upa River basin after 1986 are negligible [22, 39]. The total mass of sediments deposited on the floodplains in 1986–2018 was no more than 65 000–75 000 tons (this amount was calculated taking into account the length of permanent streams in the catchment of the Shchekino reservoir (160 km) and the average thickness of annually deposited sediments). It is generally consistent with the estimates of the input (sediment inflow from the slopes) and output (sediment accumulation in the bottom of the reservoir) parts of sediment budget.

Despite the fact that the content of  $^{137}\text{Cs}$  has almost halved in the past 30 years owing to the isotope decay, the total  $^{137}\text{Cs}$  inventory in the alluvial soils of the low floodplain in 2018 remained at the level of 1986 due to the accumulation of contaminated particles washed away from the arable land (Figs. 1b and 3e–3f) and still exceeded the maximum permissible concentration. The dominant role of sediments washed off from the arable land in sediment load of the rivers is confirmed by the high  $^{137}\text{Cs}$  content in fresh alluvial sediments of the flood in 2018 on the Upa River floodplain

near the sampling site (Fig. 1b, point 4). The  $^{137}\text{Cs}$  concentration in two samples is 353–368 kBq/kg, which corresponds to the average isotope inventory in the topsoil in the Shchekino reservoir catchment.

The  $^{137}\text{Cs}$  content in the alluvial meadow soils of the middle and high floodplains of the rivers in the Shchekino basin decreased by half in comparison with that in 1986 because of the radioactive decay of  $^{137}\text{Cs}$  and the absence of high floods with the delivery of new portions of contaminated sediments eroded from the arable land. The same tendency was observed for other rivers draining the territory of the Plavsk cesium spot [39]. An exception is a relatively rare situation, when the river valley side is plowed and the sediments washed away from this arable land are redeposited in the rear part of the river floodplain, forming a colluvial fan overlying alluvial deposits [22].

Owing to the low average annual soil loss from the arable land, which varies in the range of 1.3–1.6 t/(ha yr) depending on the type of soil, the decrease in the total  $^{137}\text{Cs}$  inventory of arable horizons caused by erosion losses averaged 1.5% of the inventory at the time of its fallout from the atmosphere in May 1986. For different soil types, it ranged from 2% for meadow chernozemic soils to 1.3% for Chernozems. On steep parts of arable slopes and in the bottoms of slope hollows, where the average annual rates of erosion exceed 10 t/(ha yr) and may reach 40 t/(ha yr) in some cases, the reduction of the  $^{137}\text{Cs}$  inventory due to the erosional soil loss reaches 12–50%. The share of such lands is no more than 0.4% of the total arable land in the catchment of the Shchekino reservoir.

It should be noted that the average annual soil loss from arable land of the Shchekino reservoir catchment in 1986–2018 is more than three times lower than the previously published calculated data for this part of Tula region [38]. A decrease in the sediment yield from 20 t/(km<sup>2</sup> yr) in the mid-1980s [33] to 6.1 t/(km<sup>2</sup> year) in 2008–2015 according to AIS GMVO [53] has favored a general decrease in the rate of soil water erosion on arable land in the Upa River basin in the recent decades. The average long-term (1986–2018) sediment yield on the basis of data on the volume of bottom sediments for the catchment of the Shchekino reservoir was 9.5 t/(km<sup>2</sup> yr).

A tendency for a decrease in the proportion of basin sediments from 1986 to 2018 was revealed from the estimates of the total soil loss from arable land and an increase in the proportion of channel sediments. It is also evidenced by data on the coarsening of the texture of bottom sediments in the Shchekino reservoir in the upper layers at all sampling points (Fig. 4).

The main part of soil material washed away from the arable land during rainstorm erosion is redeposited within colluvial fans on the unplowed lower parts of the slopes. At the same time, the maximum rates of sediment accumulation are observed in the hollow

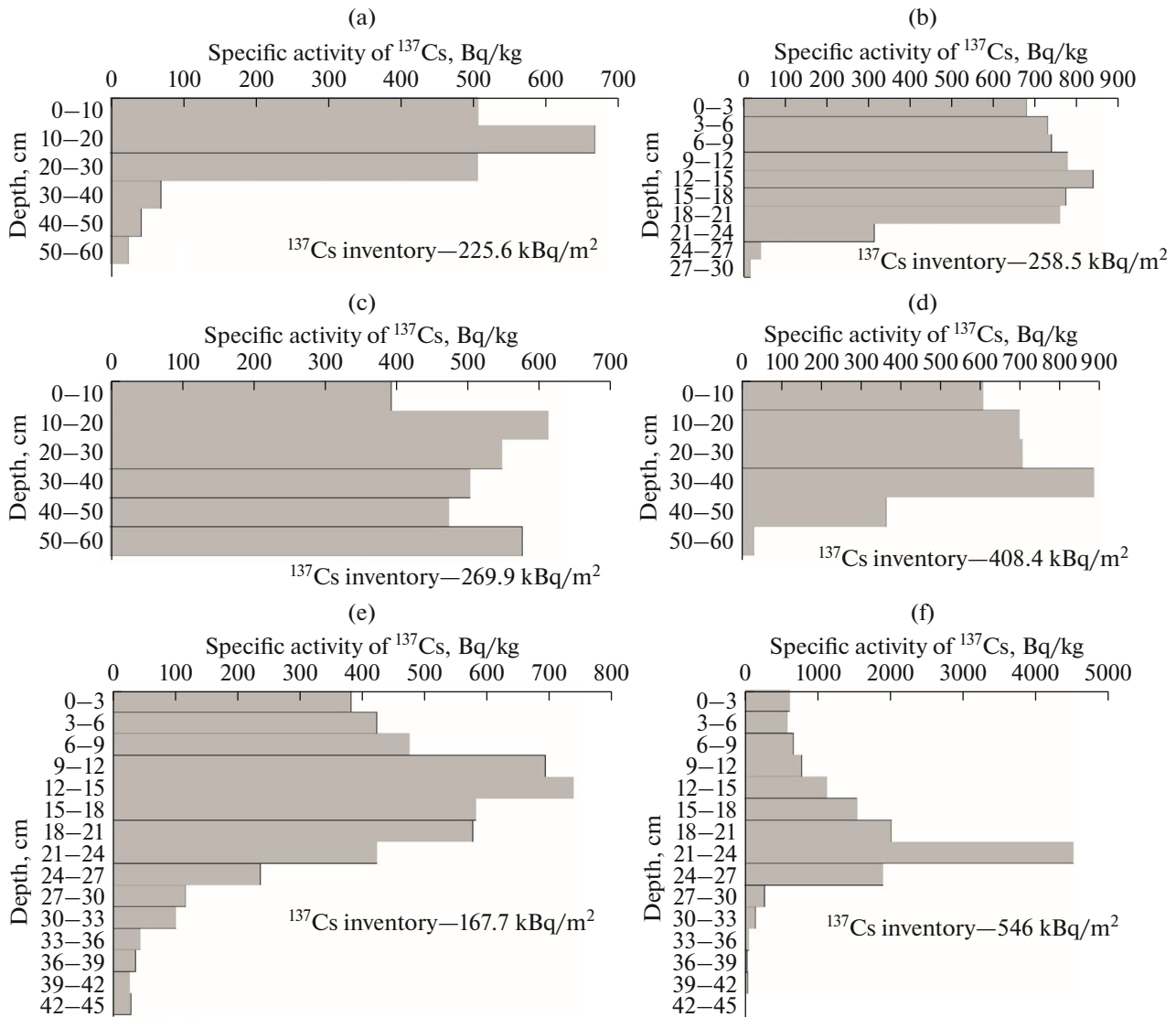


**Fig. 3.** Diagrams of the depth distribution and total <sup>137</sup>Cs inventory in the erosion (slope) and accumulation areas: (a) upper part of the slope, arable land, basin of the Lokna River, sampling in 2011; (b) middle part of the slope, arable land, Lokna River basin, sampling in 2011; (c, d) grassed part of the hollow at the top of the bottom of dry valley in the upper reaches of the Lokna River (see point 2, Fig. 1b), sampling in 2010; (e) floodplain of the Upa River (see point 4, Fig. 1b), sampling in 2018; and (f) floodplain of the Lokna River (see point 3, Fig. 1b), sampling in 2014. Data on the total <sup>137</sup>Cs inventory are given for the periods of sampling.

bottoms (Fig. S5) located outside the arable land, where the total <sup>137</sup>Cs inventory in some cases exceeds the inventory formed during its initial fallout in 1986 (Figs. 3c–3d). It should be kept in mind that such areas can be identified only during field and subsequent analytical studies because of the high spatial irregularity of rainstorm runoff, and their share is no more than 1% of the total catchment area of the Shchekino reservoir.

Only during extremely heavy rainfalls, which contribute to the formation of temporary streams in dry valleys, as observed in the bottom of dry valley Chasovenkov Verkh (the Lokna River basin) [21], a fairly significant part of washed away sediment is redeposited in their bottoms, and is also transported to permanent streams.

At the same time, during the formation of snowmelt runoff, sediment redeposition along the way of runoff flows from arable land to permanent streams occurs more evenly due to a higher water discharges and lower turbidity of temporary streams [14]. As a result, most sediments washed away from the arable land during the snowmelt season but not entering the river channels, are redeposited in the bottoms of dry valleys. The rate of sediment accumulation in the bottom of each dry valley is controlled by its morphology (presence of a secondary incision, width, slope) and rate of the meltwater flow. Available data attest to a general decrease in the rate of sediment redeposition in the bottoms of the dry hollows in the Central Russian Upland after 1986 by almost an order of magni-

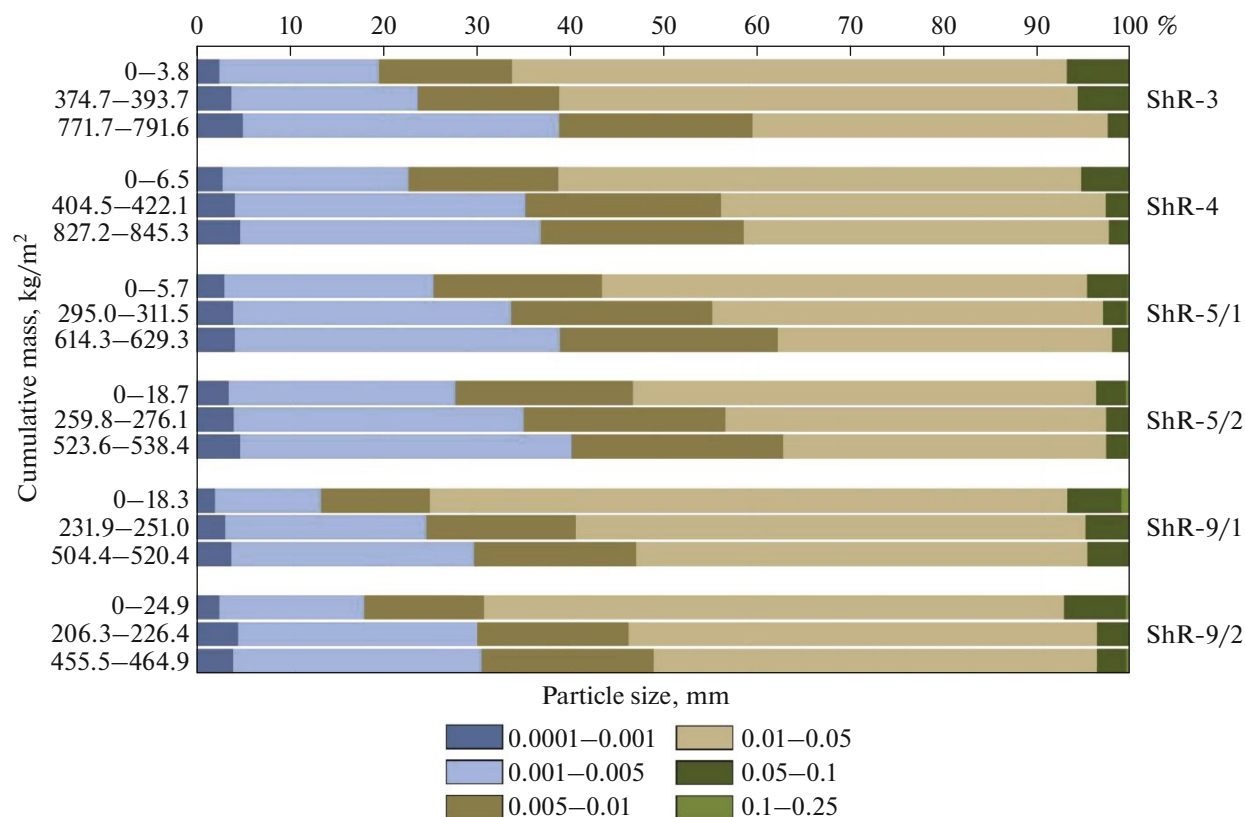


**Fig. 4.** Changes in the particle size distribution of bottom sediments by depth (cumulative mass) at sampling points in different parts of the Shchekino reservoir (see Fig. 1c).

tude compared with 1963–1986 [34]. Thus, an increase in the  $^{137}\text{Cs}$  inventory in the layered soils (stratozems) of the bottoms of dry valleys due to the deposition of contaminated sediments delivered from the arable land does not compensate for the decrease in the  $^{137}\text{Cs}$  content under the impact of radioactive decay. At the same time, the total  $^{137}\text{Cs}$  inventory in the bottoms of dry valleys remains 25–40% higher than that in the soils of arable lands and uncultivated areas on interfluvies of the Shchekino reservoir catchment (fallow lands, forests, shrubs, etc.).

## CONCLUSIONS

Studies of the redistribution of soil particles washed away from arable land during the snowmelt and rain-storm erosion along the transportation path to permanent streams and water reservoirs of the Shchekino reservoir catchment over the period from the fallout of  $^{137}\text{Cs}$  of Chernobyl origin in early May 1986 to the end of 2018 were carried out. Their results made it possible to quantitatively assess changes in the  $^{137}\text{Cs}$  content in soils of various types in the areas of the loss and accumulation of sediments. On arable land, the decrease in the total  $^{137}\text{Cs}$  inventory caused by the soil washing off averaged 1.5–2% of its actual inventory, which

decreased by more than two times in comparison with the inventory in May 1986 due to natural decay. However, on 0.4% of the arable land, where the runoff rate is maximum due to the relatively steep slopes and runoff concentration along the hollows, the  $^{137}\text{Cs}$  inventory decreased by 12–40%. More than 90% of soil particles washed away from arable land and  $^{137}\text{Cs}$  transported with them were redeposited along the transportation pathways from slopes to permanent streams.

The maximum rates of sediment accumulation are noted in the bottoms of slope hollows in areas from the lower edge of arable land to the upper reaches of dry first-order valleys. Owing to the high rates of sediment accumulation in these zones, the total  $^{137}\text{Cs}$  inventory in their soils often even exceed the values recorded after the  $^{137}\text{Cs}$  fallout in May 1986. Other areas of  $^{137}\text{Cs}$  accumulation are the bottoms of dry valleys (balkas), where layered soils—stratozems—are developed, the foots of plowed slopes, and the low floodplains of rivers. In these areas, the total  $^{137}\text{Cs}$  inventory still exceeds the lower limit of permissible radioactive contamination of soils (37 kBq/m<sup>2</sup>) [2]. This is due to the regular deposition of contaminated soil material washed away from arable land, which compensates for the decrease in the total  $^{137}\text{Cs}$  inventory due to radio-

active decay. Thus, the areas of distribution of stratozems and alluvial soddy soils on the low floodplains are the areas of maximum  $^{137}\text{Cs}$  accumulation within the catchment of the Shchekino reservoir.

The obtained estimates of the redistribution of sediments and  $^{137}\text{Cs}$  during their transportation from arable land to the channels of permanent streams are in agreement with our data on the accumulation of bottom sediments in the Shchekino reservoir. Moreover, the revealed trend of a decrease in the annual erosional soil loss in 1986–2018 caused by a decrease in the snowmelt erosion, and, hence, a decrease in the share of basin sediments in the composition of bottom sediments in the reservoir is confirmed by the coarsening of the texture of the upper layers of the bottom sediments in the reservoir, as well as by a more than three-fold decrease in sediment discharge into the Upa River per unit area after 2008 in comparison with the long-term average values before 1985.

#### ACKNOWLEDGMENTS

The authors would like to thank the General Director of the Shchekinskaya Electric Power Station A.V. Karpunin for providing a bathymetric map of the Shchekino reservoir and Ph.D. A.L. Gurinov and Ph.D. N.V. Kuzmenkova for participation in fieldwork on sampling bottom sediments.

#### FUNDING

This study was carried out in agreement with the state assignment of the Makkaveev Laboratory of Soil Erosion and Fluvial Processes at the Faculty of Geography of Lomonosov Moscow State University (registration no. AAAA-A16-116032810084-0) and partly supported by the Russian Foundation for Basic Research (project no. 18-55-50002 yaf )

#### CONFLICT OF INTEREST

The authors declare that they have no conflict of interest.

#### SUPPLEMENTARY INFORMATION

The online version contains supplementary material available at <https://doi.org/10.1134/S106422932102006X>.

**Table S1.** Crop and management factor ( $C$ ) values for various land use types and underlying surface [15, 23, 44].

Equations for calculating soil erodibility coefficient.

**Table S2.** The main soil types of the Verkhnyaya Upa River basin, their texture and erodibility (factor  $K$ ).

**Fig. S3.** Trends of changes in the maximum water levels of spring floods (Tula hydrological station) and in the soil freezing depth on arable land (Plavsk weather station) for 1987–2018.

**Fig. S4.** Changes in the amount of liquid precipitation and the rainfall erosivity according to data of the Plavsk weather station from 1963 to 2018 (by 1]).

**Table S4.** The main statistical characteristics of rainfall erosivity ( $R$ ), MJ mm/(h ha yr), calculated according to [40] from data of the Plavsk weather station [1].

**Fig. S5.** Scheme of sediment accumulation zones within a small plowed catchment.

#### REFERENCES

- O. N. Bulygina, V. N. Razuvaev, N. N. Korshunova, and N. V. Shvets, Automated information system for processing regime information (AISORI). <http://aisori.meteo.ru/ClimateR>.
- R. M. Aleksakhin, "Radioactive contamination as a type of soil degradation," *Eurasian Soil Sci.* **42**, 1386–1396 (2009).
- V. S. Anisimov, N. I. Sanzharova, and R. M. Aleksakhin, "The forms of occurrence and vertical distribution of  $^{137}\text{Cs}$  in soils in the accident zone of the Chernobyl nuclear power plant, *Pochvovedenie*, No. 9, 31–40 (1991).
- The Atlas of Recent and Predictable Consequences of Chernobyl Accident on Polluted Territories of Russia and Belarus* (ARPA Russia-Belarus, Moscow, 2009) [in Russian].
- I. D. Braude, "Nature of spotty patterns of arable soils on slopes and their melioration," *Pochvovedenie*, No. 12, 89–97 (1991).
- V. P. Gerasimenko, "Water erosion of soils in various regions of the European part of the Soviet Union," *Pochvovedenie*, No. 12, 96–109 (1987).
- V. N. Golosov, "Erosive-accumulative processes and sediment budget in the Protva River basin," *Vestn. Mosk. Univ., Ser. 5: Geogr.*, No. 6, 19–25 (1988).
- A. M. Grin, "Stationary studies of runoff and soil washing processes," in *Modern Exogenic Processes of Relief Development* (Nauka, Moscow, 1970), pp. 89–95.
- Unified State Register of Soil Resources of Russia*. <http://atlas.mcx.ru/materials/egrpr/content/1sem.html>.
- M. A. Ivanov, A. V. Prishchepov, V. N. Golosov, E. E. Zalyaliev, K. V. Efimov, A. A. Kondrat'eva, A. D. Kinyashova, and Yu. K. Ionova, "Mapping of the dynamics of arable lands in the river basins of the European part of Russia in 1985–2015," *Sovrem. Probl. Distantionnogo Zondirovaniya Zemli Kosm.* **14** (5), 161–171 (2017).
- M. M. Ivanov, A. L. Gurinov, N. N. Ivanova, A. V. Konoplev, E. A. Konstantinov, N. V. Kuz'menkova, E. V. Terskaya, and V. N. Golosov, "Dynamics of  $^{137}\text{Cs}$  accumulation in the bottom sediments of the Shekino Reservoir during post-Chernobyl period," *Radiats. Biol., Radioekol.* **59** (6), 651–663 (2019).
- G. A. Larionov, *Erosion and Deflation of Soils: General Patterns and Quantitative Assessment* (Moscow State Univ., Moscow, 1993) [in Russian].
- L. F. Litvin, *Geography of Erosion of Agricultural Soils in Russia* (Akademkniga, Moscow, 2002) [in Russian].
- L. F. Litvin, V. N. Golosov, N. G. Dobrovolskaya, N. I. Ivanova, Z. P. Kiryukhina, and S. F. Krasnov, "Stationary studies of soil erosion during snow melting in the central nonchernozemic region," in *Soil Erosion*

- and Channel Processes* (Moscow State Univ., Moscow, 1998), Vol. 11, pp. 57–76.
15. L. F. Litvin, Z. P. Kiryukhina, S. F. Krasnov, and N. G. Dobrovolskaya, “Dynamics of agricultural soil erosion in European Russia,” *Eurasian Soil Sci.* **50**, 1344–1353.
  16. A. I. Ratnikov, “Geomorphological and agropedogenic regions of Tula oblast,” in *Soil Zonation of USSR* (Moscow State Univ., Moscow, 1960), pp. 92–115.
  17. A. Yu. Sidorchuk, “Sediment balance in erosional-channel systems,” *Geomorfologiya*, No. 1, 14–21 (2015).
  18. A. V. Khristoforov, N. M. Yumina, and P. A. Belyakova, “A day-before forecast of rainstorm floods for of rivers of the Black Sea coast of the Caucasus,” *Vestn. Mosk. Univ., Ser. 5: Geogr.*, No. 3, 50–57 (2015).
  19. E. N. Shamshurina, V. N. Golosov, and M. M. Ivanov, “Spatiotemporal reconstruction of the deposition of Chernobyl <sup>137</sup>Cs on the soil cover in the upper reaches of the Lokna River basin,” *Radiats. Biol., Radioekol.*, No. 4, 414–425 (2016).
  20. A. T. Barabanov, S. V. Dolgov, N. I. Koronkevich, V. I. Panov, and A. I. Petel’ko, “Surface runoff and snowmelt infiltration into the soil on plowlands in the forest-steppe and steppe zones of the East European Plain,” *Eurasian Soil Sci.* **1**, 66–72 (2018).
  21. V. R. Belyaev, V. N. Golosov, K. S. Kislenko, J. S. Kuznetsova, and M. V. Markelov, “Combining direct observations, modeling, and <sup>137</sup>Cs tracer for evaluating individual event contribution to long-term sediment budgets,” in *Sediment Dynamics and the Hydromorphology of Fluvial Systems*, IAHS Publication no. 325 (International Association of Hydrological Sciences, Wallingford, 2008), pp. 114–122.
  22. V. R. Belyaev, V. N. Golosov, M. V. Markelov, O. Evrard, N. N. Ivanova, T. A. Paramonova, and E. N. Shamshurina, “Using Chernobyl-derived <sup>137</sup>Cs to document recent sediment deposition rates on the River Plava floodplain (Central European Russia),” *Hydrol. Process.* **27**, 807–821 (2013).
  23. R. Benavidez, B. Jackson, D. Maxwell, and K. Norton, “A review of the (Revised) Universal Soil Loss Equation ((R)USLE): with a view to increasing its global applicability and improving soil loss estimates,” *Hydrol. Earth Syst. Sci.* **22** (11), 6059–6086 (2018). <https://doi.org/10.5194/hess-22-6059-2018>
  24. L. Borselli, P. Cassi, and D. Torri, “Prolegomena to sediment and flow connectivity in the landscape: a GIS and field numerical assessment,” *Catena* **75** (3), 268–277 (2008). <https://doi.org/10.1016/j.catena.2008.07.006>
  25. M. Bossard, J. Feranec, and J. Otahel, *CORINE Land Cover Technical Guide—Addendum 2000: Technical Report No. 40* (European Environmental Agency, Copenhagen, 2000). <http://terrestrial.eionet.eu.int>.
  26. G. Buttner, J. Feranec, G. Jaffrain, L. Mari, G. Maucha, and T. Soukup, “The CORINE land cover 2000 project,” *EARSeL Proc.* **3** (3), 331–346 (2004).
  27. O. Conrad, B. Bechtel, M. Bock, H. Dietrich, E. Fischer, L. Gerlitz, J. Wehberg, V. Wichmann, and J. Böhrner, “System for Automated Geoscientific Analyses (SAGA) v. 2.1.4,” *Geosci. Model Dev.* **8** (7), 1991–2007 (2015). <https://doi.org/10.5194/gmd-8-1991-2015>
  28. M. De Cort, G. Dubois, Sh. D. Fridman, M. G. Germenchuk, Yu. A. Izrael, A. Janssens, A. R. Jones, G. N. Kelly, E. V. Kvasnikova, I. I. Matveenkov, I. M. Nazarov, Yu. M. Pokumeiko, V. A. Sitak, E. D. Stukin, L. Ya. Tabachny, Yu. S. Tsaturov, and S. I. Avdyushin, *Atlas of Cesium Deposition on Europe after the Chernobyl Accident: European Commission Report EUR 16733* (European Commission, Luxembourg, 1998).
  29. M. Delmas, L. T. Pak, O. Cerdan, V. Souchère, Y. Le Bissonnais, A. Couturier, and L. Sorel, “Erosion and sediment budget across scale: a case study in a catchment of the European loess belt,” *J. Hydrol.* **420–421**, 255–263 (2012). <https://doi.org/10.1016/j.jhydrol.2011.12.008>
  30. P. Desmet and G. Govers, “A GIS procedure for automatically calculating the USLE LS factor on topographically complex landscape units,” *J. Soil Water Conserv.* **51** (5), 427–433 (1996).
  31. O. Evrard, J. P. Laceyby, H. Lepage, Y. Onda, O. Cerdan, and S. Ayrault, “Radiocesium transfer from hillslopes to the Pacific Ocean after the Fukushima Nuclear Power Plant accident: a review,” *J. Environ. Radioact.* **148**, 92–110 (2015).
  32. V. N. Golosov, “Special considerations for areas affected by Chernobyl fallout,” in *Handbook for the Assessment of Soil Erosion and Sedimentation Using Environmental Radionuclides* (Kluwer, Dordrecht, 2002), pp. 165–183.
  33. V. N. Golosov, “Influence of different factors on the sediment yield of the Oka basin rivers (central Russia),” in *Sediment Dynamics and the Hydromorphology of Fluvial Systems*, IAHS Publication no. 306 (International Association of Hydrological Sciences, Wallingford, 2006), pp. 28–36.
  34. V. N. Golosov, N. N. Ivanova, A. V. Gusarov, and A. G. Sharifullin, “Assessment of the trend of degradation of arable soils on the basis of data on the rate of stratozem development obtained with the use of <sup>137</sup>Cs as a Chronomarker,” *Eurasian Soil Sci.* **50**, 1195–1208 (2017).
  35. M. A. Komissarov and S. Ogura, “Distribution and migration of radiocesium in sloping landscapes three years after the Fukushima-1 nuclear accident,” *Eurasian Soil Sci.* **50**, 861–871 (2017). <https://doi.org/10.1134/S1064229317070043>
  36. A. Konoplev, Y. Wakiyama, T. Wada, V. Golosov, K. Nanba, and T. Takase, “Radiocesium in ponds of the proximity to the Fukushima Daiichi NPP,” *Water Res.* **45**, 589–597 (2018).
  37. V. G. Linnik, I. V. Mironenko, N. I. Volkova, and A. V. Sokolov, “Landscape–biogeochemical factors of transformation of the Cs-137 contamination field in the Bryansk region,” *Geochem. Int.* **55**, 887–901 (2017).
  38. K. A. Maltsev and O. P. Yermolaev, “Potential soil loss from erosion on arable lands in the European part of Russia,” *Eurasian Soil Sci.* **52**, 1588–1597 (2019).
  39. S. V. Mamikhin, V. N. Golosov, T. A. Paramonova, E. N. Shamshurina, and M. M. Ivanov, “Vertical distribution of <sup>137</sup>Cs in alluvial soils of the Lokna River

- floodplain (Tula oblast) long after the Chernobyl accident and its simulation," *Eurasian Soil Sci.* **49**, 1432–1442 (2016).  
<https://doi.org/10.1134/S1064229316120103>
40. V. Naipal, C. Reick, J. Pongratz, and K. van Oost, "Improving the global applicability of the RUSLE model—Adjustment of the topographical and rainfall erosivity factors," *Geosci. Model Dev.* **8** (9), 2893–2913 (2015).  
<https://doi.org/10.5194/gmd-8-2893-2015>
  41. M. H. Paller, G. T. Jannik, and P. D. Fledderman, "Changes in <sup>137</sup>Cs concentrations in soil and vegetation on the floodplain of the Savannah River over a 30 year period," *J. Environ. Radioact.* **99**, 1302–1310 (2008).  
<https://doi.org/10.1016/j.jenvrad.2008.04.001>
  42. P. Panagos, P. Borelli, K. Meusburger, B. Yu, A. Klik, K. J. Lim, J. E. Yang, et al., "Global rainfall erosivity assessment based on high-temporal resolution rainfall records," *Sci. Rep.* **7**, 4175 (2017).  
<https://doi.org/10.1038/s41598-017-04282-8>
  43. P. Panagos, P. Borrelli, and K. Meusburger, "A new European slope length and steepness factor (LS-factor) for modeling soil erosion by water," *Geosciences* **5**, 117–126 (2015).  
<https://doi.org/10.3390/geosciences5020117>
  44. P. Panagos, P. Borrelli, K. Meusburger, C. Alewell, E. Lugato, and L. Montanarella, "Estimating the soil erosion cover-management factor at the European scale," *Land Use Policy* **48**, 38–50 (2015).  
<https://doi.org/10.1016/j.landusepol.2015.05.021>
  45. M. C. Peel, B. L. Finlayson, and T. A. McMahon, "Updated world map of the Köppen-Geiger climate classification," *Hydrol. Earth Syst. Sci.* **11**, 1633–1644 (2007).
  46. K. G. Renard, G. R. Foster, G. A. Weesies, D. K. McCool, and D. C. Yoder, *Predicting Soil Erosion by Water: A Guide to Conservation Planning with the Revised Universal Soil Loss Equation (RUSLE)*, Agricultural Handbook no. 703 (US Governmental Printing Office, Washington, DC, 1997), p. 404. <https://doi.org/DC0-16-048938-5> 65–100.
  47. A. Varley, A. Tyler, Y. Bondar, A. Hosseini, V. Zabrotski, and M. Dowdall, "Reconstructing the deposition environment and long-term fate of Chernobyl <sup>137</sup>Cs at the floodplain scale through mobile gamma spectrometry," *Environ. Pollut.* **240**, 191–199 (2018).
  48. O. Vigiak, L. Borselli, L. T. H. Newham, J. McInnes, and A. M. Roberts, "Comparison of conceptual landscape metrics to define hillslope-scale sediment delivery ratio," *Geomorphology* **138** (1), 74–88 (2012).  
<https://doi.org/10.1016/j.geomorph.2011.08.026>
  49. L. Wang and H. Liu, "An efficient method for identifying and filling surface depressions in digital elevation models for hydrologic analysis and modeling," *Int. J. Geogr. Inf. Sci.* **20** (2), 193–213 (2006).  
<https://doi.org/10.1080/13658810500433453>
  50. J. R. Williams, "The EPIC model," in *Computer Models of Watershed Hydrology*, Ed. by V. P. Singh (Water Resources, Highlands Ranch, CO, 1995), chap. 25, pp. 909–1000.
  51. W. H. Wischmeier, D. D. Smith, and R. E. Uhland, "Evaluation of factors in the soil loss equation," *Agric. Eng.* **39** (8), 458–462 (1958).
  52. S. Wu, J. Li, and G. Huang, "An evaluation of grid size uncertainty in empirical soil loss modeling with digital elevation models," *Environ. Model. Assess.* **10** (1), 33–42 (2005).
  53. Automated information system for state monitoring of water bodies. <https://gmvo.skniivh.ru>.
  54. ALOS Global Digital Surface Model: ALOS World 3D–30m (AW3D30). <https://www.eorc.jaxa.jp/ALOS/en/aw3d30/index.htm>.

*Translated by V. Klyueva*